

Three-dimensional structure of tundra vegetation cover dominated by sedges

IV Matelenok¹, VV Melentyev¹

¹ St Petersburg State University of Aerospace Instrumentation (Saint Petersburg, Russian Federation)

Corresponding author: Igor Matelenok (igor_matelenok@mail.ru)

Academic editor: Aleksandr I. Malov ♦ **Received** 4 June 2018 ♦ **Accepted** 13 November 2018 ♦ **Published** 14 December 2018

Citation: Matelenok IV, Melentyev VV (2018) Three-dimensional structure of tundra vegetation cover dominated by sedges. Arctic Environmental Research 18(4): 132–140. <https://doi.org/10.3897/issn2541-8416.2018.18.4.132>

Abstract

Modelling of radiation transfer through natural multilayer media is relevant for many climatological, hydrological and ecological issues. The possibility of using the models is determined by the comprehensiveness of the information on the properties and structure of certain layers: ground, vegetation, atmosphere. Three-dimensional spatial organisation of tundra vegetation cover is understudied compared to vegetation structure of the boreal zone. In the scope of the research, the structure of sedge-tundra vegetation cover in the Nenets Autonomous Area and the Murmansk Region was investigated using specialised hardware-software system which allows to take photos of the cover from different angles, construct virtual three-dimensional models and obtain the values of parameters characterising the structure. The field survey of the sites was carried out in August 2016 and 2017. Phytoelement angle distributions obtained differ from standard erectophile distribution frequently used for modelling orientation of phytoelements in cover formed by grasses/sedges. The shape of phytoelement angle distribution varies from site to site depending on the dominant species. Experiments on fitting real distributions by different functions established that the generalised shape of the distribution in the studied cover is best described by a rotated-ellipsoidal function with a parameter equal to 2.69. Information obtained on the structure of the vegetation cover can be used in modelling microwaves and solar radiation propagation.

Keywords

Arctic, leaf angle distribution, radiation transfer, remote sensing, three-dimensional structure, tundra ecosystems, vegetation cover

Introduction

Modelling of the matter and energy balance in the ground-vegetation-atmosphere system is a key goal in the context of estimating and forecasting the environmental state and requires as much information as possible on the structure and properties of each of the system components. The available data on the vegetation cover structure make it possible to describe solar radiation propagation and the biomass accumulation process and establish a relationship between the reflectance and the biophysical parameters of the vegetation. This information is also needed to solve other problems, i.e., to retrieve the soil temperature and moisture from microwave remote sensing data using models of radiation transfer in multilayer scattering media (Jackson and Schmugge 1991, Huang et al. 2016).

Only a few studies are now focused on vegetation cover structure on the territories to the north of 60° N (for example, Greaves et al. 2015, Magney et al. 2016). Among the most recent publications on this topic, studies (Zou et al. 2014, Juszak et al. 2014, 2017) deserve special mention. One of the basic tasks of these studies is to estimate leaf angle distribution by means of a photographic method proposed by (Pisek et al. 2011).

The objective of this study is to obtain data on the 3D structure of vegetation cover of the south sedge tundra in Russia’s western Arctic, as well as of floodplains of the same location. The following tasks had to be fulfilled to achieve this goal:

- 1) develop and implement new approaches to vegetation cover structure studies by means of a special-purpose hardware and software system (HSS),
- 2) select representative areas in the south tundra subzone occupied by several widespread complexes of plant communities,
- 3) perform a field survey within these communities,
- 4) calculate structure parameters and obtain spatial models of the cover fragments using the data of the field survey.

Field sites

The sites under study are located on the territory of the Nenets Autonomous Area (U2016-1, U2016-3 and U2016-8) and the Murmansk Region (U2017-2, U2017-3, U2017-5) – Fig. 1. The index assigned to each site reflects the year of its field survey and its sequence

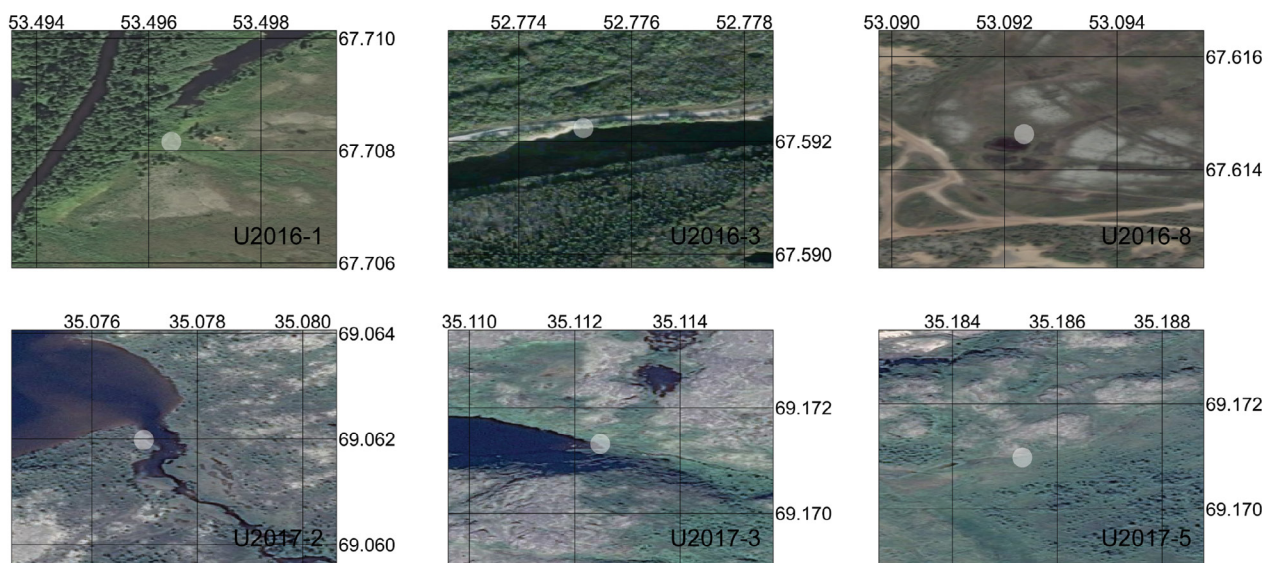


Fig. 1. Location of the sites on the territory of the Nenets Autonomous Area (U2016-1, U2016-3 and U2016-8) and the Murmansk Region (U2017-2, U2017-3, U2017-5)

number among the sites surveyed during that year. Sites more than 700km apart and belonging to different floristic areas have been selected in order to identify regional differences in the vegetation cover. A brief description of the sites is provided below and in Table 1.

U2016-1. Valley of the Pyatumboi river. Cotton-grass-sedge-moss community of bottomlands (dominant species – *Carex rariflora*, *Equisetum palustre*, *Sphagnum balticum*, other species – *Eriophorum angustifolium*, *Vaccinium uliginosum*, *Salix phylicifolia*).

U2016-3. The bank of the bayou of the Gorodetsky Shar branch, valley of the Pechora river. Herb-sedge meadow community, the poium lower level (dominant species – *Carex aquatilis*, *Colpodium fulvum*, other species – *Phalaroides arundinacea*, *Calamagrostis langsdorffii*, *Poa arctica*).

U2016-8. Flat palsa bog. Herb-dwarf-shrub-moss-lichen community (dominant species – *Carex rariflora*, *Eriophorum russeolum*, *Sphagnum balticum*, other species – *Vaccinium uliginosum*, *Cladonia rangiferina*, *Betula nana*).

U2017-2. Sobachy stream bank. Herb-dwarf-shrub-moss community in the minor stream valley (dominant species – *Carex rotundata*, *Carex aquatilis*, other species – *Salix lapponum*, *Vaccinium uliginosum*, *Sphagnum russowii*, *Betula nana*).

U2017-3. Lake bank. Herb-dwarf-shrub-moss community (dominant species – *Carex aquatilis*, *Rubus chamaemorus*, other species – *Vaccinium uliginosum*, *Empetrum hermaphroditum*, *Betula nana*).

U2017-5. Moist bottomland. Cotton-grass-sedge-moss community (dominant species – *Carex rariflora*, *Eriophorum angustifolium*, other species – *Salix lapponum*, *Sphagnum russowii*).

Overview photos of the vegetation cover at the sites are shown in Fig. 2.

The wind speed on the dates of the field survey (Table 1) according to the closest meteorological stations did not exceed 3–5m/s. There was no precipitation at the study sites within the 12 hours before the survey and precipitated water did not impact on the position of the phytoclements. In order to produce the sample of required size, the assessment of the structure parameters was performed for at least 12 fragments of the vegetation cover within each site.

Materials and methods

In order to obtain initial data on the cover structure and to perform detailed analysis of them, we used the system developed in 2015 at the laboratory for



Fig. 2. Vegetation cover at the sites under study

Table 1. Location and survey dates for sites located on the territory of the Nenets Autonomous Area and the Murmansk Region

Site	Site centre coordinates	Survey date
U2016-1	67.708156° N, 53.496402° E	6 August 2016
U2016-3	67.592236° N, 52.775145° E	7 August 2016
U2016-8	67.614631° N, 53.092349° E	8 August 2016
U2017-2	69.061983° N, 35.076983° E	7 August 2017
U2017-3	69.171317° N, 35.112483° E	8 August 2017
U2017-5	69.170983° N, 35.185333° E	10 August 2017

monitoring and control of natural-engineering systems of St. Petersburg State University of Aerospace Instrumentation (Matelenok and Melentyev 2016). The hardware and software system (HSS) consists of a frame, background surface, photo/video camera, laptop with specially developed software, data cables, bubble level and compass. This system takes pictures of the vegetation cover fragments from different angles (generally 4–7 camera positions are used), calcu-

lates the parameters of the structure and creates 3D models of the cover fragments. The dimension of the vegetation fragment enveloped by the instrument is 0.8m^2 (this bounded volume resembles a cylinder). The HSS may be used for surveying medium dense canopies with plants of 10–50cm height (Matelenok and Melentyev 2018). A photograph of the system ready to operate is given in Fig. 3. In 2016–2017, the HSS was upgraded in order to expand its functionality and improve the speed of software. Core code blocks of the program are written in languages M and R. The graphical interface of the final version of the software at one stage of processing data from the camera is shown in Fig. 4.

The values of the vegetation cover structure parameters are assessed by the software module designed to identify objects with one large and two small characteristic dimensions (linear). Here, the photographs of the cover fragment are processed following the algorithm:



Fig. 3. The hardware and software system (without PC) placed on the ground during vegetation structure survey

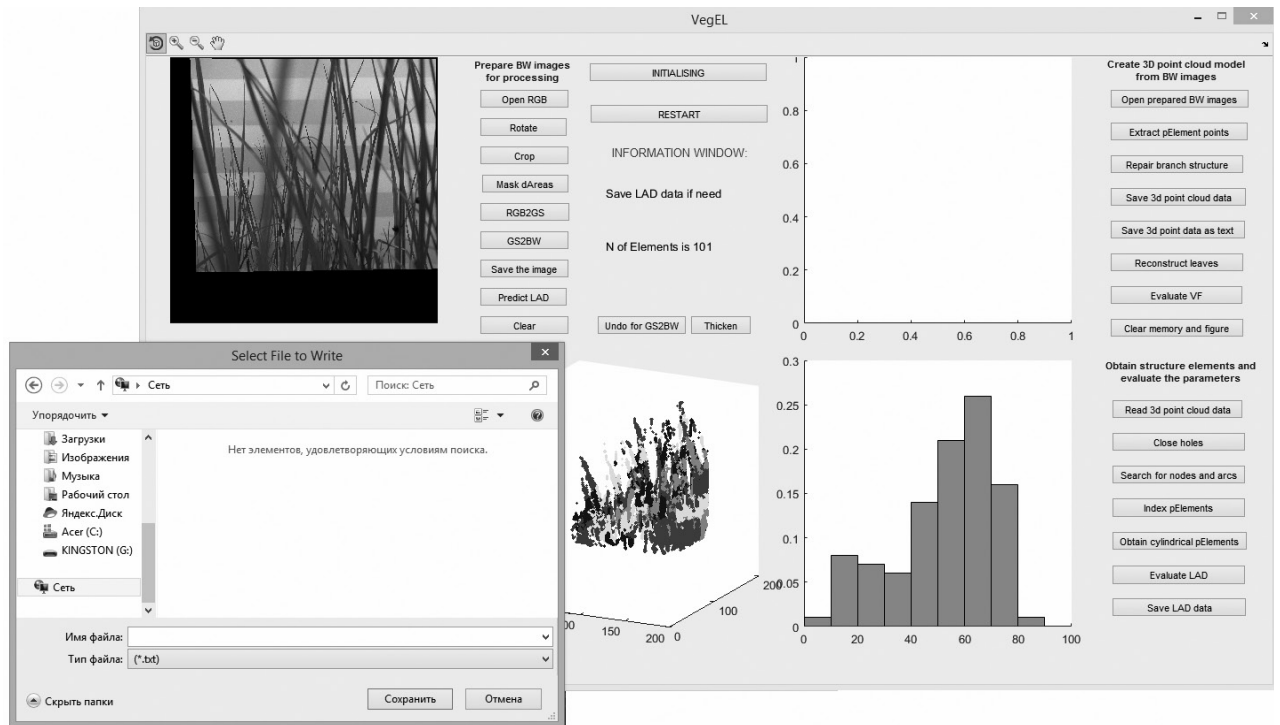


Fig. 4. General view of the main window of the software graphical interface of the vegetation 3D structure survey system

1. The photographs are pre-processed (distortions are corrected, some background areas preventing automated detection of phytoelements are interactively masked).
2. A point cloud is created using a projection theory based on the fragment photographs taken from several angles, then this cloud is cleared and the missing data is reconstructed.
3. A skeletal structure is extracted from the point cloud, points of interest of phytoelements and their components (branching points and end points) with specific orientation are identified.
4. The point cloud is classified by the minimum weighted Euclidean distance classification method.
5. The values of coordinates and angles determining orientation of phytoelements are assessed, histograms of incidence angle θ distribution are prepared (with weighting frequencies with phytoelements length, Fig. 5).
6. Virtual polygonal models of the cover fragment are created based on the phytoelements collocation data.

The HSS module has been tested for operation with linear phytoelements using an AutoCAD test virtual model, which is a polygonal structure of several phytoelements combined with a system of cameras. Setting of orientation of the phytoelements with respect to the horizon to specific angle values is achieved by rotating the model about the axes of the conditional coordinate system. A collection of views from virtual cameras at various positions of the phytoelements was saved to graphical files and used as the input test data for the HSS testing.

The tests showed that the software underestimates the inclination angles in the range of medium and high θ (the maximum deviation was 12°). In order to reduce the differences between the obtained θ and the actual angle values, during processing of the field data, they were additionally corrected using a linear model (Fig. 5) described by formula $\theta_{fit} = 1.056 \cdot \theta_{retr} + 2.096$ ($R^2 = 0.98$) and ensuring the residual $\Delta = \theta_{meas} - \theta_{fit}$ within the range from -6.6° to 7.2° . θ_{meas} are angle values measured directly, θ_{retr} are angle values reconstructed using the above-mentioned algorithm, θ_{fit} are corrected (final) values (hereinafter $\theta = \theta_{fit}$).

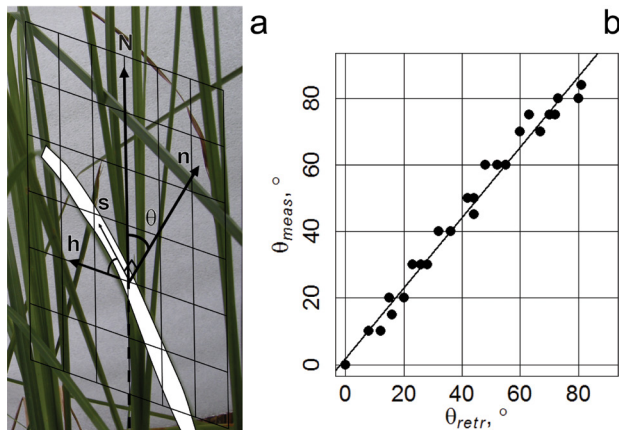


Fig. 5. Outline of measuring schema used to obtain values of phytoelement inclination angle (θ – phytoelement inclination angle, N – zenith, n – leaf surface normal, s – major leaf axis, h – projection of the major leaf axis on a horizontal plane) (a) and scatterplot of the measured (θ_{meas}) and retrieved (θ_{retr}) values of θ with fitting line (b)

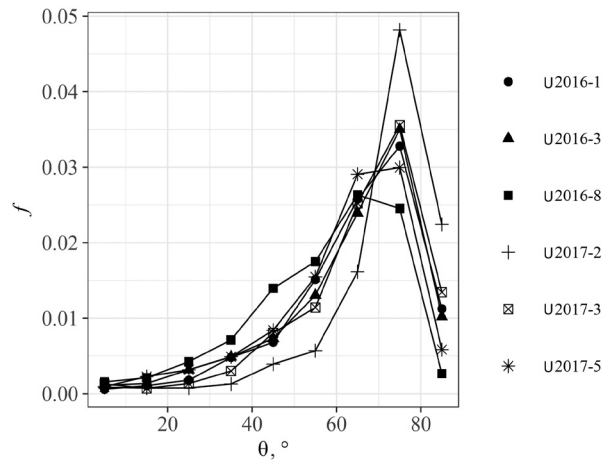


Fig. 6. Phytoelement angle (θ) distribution in the sedge-dwarf-shrub layer of the vegetation cover at investigated sites of the Nenets Autonomous Area (U2016-1, U2016-3 and U2016-8) and the Murmansk Region (U2017-2, U2017-3, U2017-5) in the form of probability density plots $f(\theta)$

Results

The field survey and processing of photographic data using the HSS for all cover fragments, which met the quality requirements (from 10 to 14 depending upon the site), provided data on phytoelement length, numerical assessments of phytoelement angle distribution and coordinates of basic points.

The longest phytoelements are registered at sites U2016-3 and U2017-3, in the sedge-dwarf-shrub layer of the vegetation cover, which is dominated by *Carex aquatilis* sedges. Other sites are characterised by smaller sizes of leaves and stems (and a thinner cover), and *Carex rotundata* and *Carex rariflora* sedges are dominant within these sites.

The sites differ in the dominant orientation of phytoelements (Fig. 6). In all cases, significant quantities of leaves and stems which position being close to vertical are observed.

The largest number of phytoelements in the range of angles from 70° to 90° is observed at site U2017-2, where the sedge-dwarf-shrub layer is dominated by *Carex rotundata* and *Carex aquatilis* and the vegetation height is small. The sites dominated by *Carex rariflora* and species of *Eriophorum* genus (U2016-8, U2017-5) are characterised by a flat (low-pitched) distribution curve. Other sites (U2016-3, U2017-3, covered with *Carex aquatilis*, and U2016-1 dominated by *Carex rariflora* sedge with inclusions of *Equisetum*), occupy an intermediate position between the two mentioned sites in terms of distribution shape.

χ^2 -test was used to confirm the assumption that the obtained phytoelement angle distributions are close to some standard theoretical distributions. The mentioned statistical values are shown in Table 2. In cases marked with an asterisk *, the hypothesis on the absence of difference between the actual and standard distribution may be rejected with an error

Table 2. Chi-square values reflecting the similarity between phytoelement angle distributions and standard distributions obtained for some sites

Type of distribution	U2016-1	U2016-3	U2016-8	U2017-2	U2017-3	U2017-5
erectophile	27.0*	19.7	18.9	25.7*	17.0	19.6
spherical	47.8*	28.2*	19.2	40.2*	23.2*	24.8*

Note. * corresponds to cases with $p < 0.01$

probability of 0.01, i.e. in such a case the similarity between the obtained phytoelement angle distribution and the certain standard distribution is little.

The generalised distribution reflecting the entire set of angle data from six sites was approximated using functions that are traditionally used for this purpose and describe both standard distributions (planophile, erectophile, plagiophile, extremophile) and transient types, which differ in shape (Wang et al. 2007). By means of comparison between the approximation results according to χ^2 test values, it was concluded that the data are best described by a rotated ellipsoidal angle density function proposed in (Thomas and Winner 2000):

$$f(\theta) = \frac{2\chi^3 \cos \theta}{\Lambda(\sin^2 \theta + \chi^2 \cos^2 \theta)},$$

$$\Lambda = \chi + 1,774(\chi + 1,182)^{-0,733},$$

where $\chi = 2.69$.

θ is the leaf angle, χ is the ratio of horizontal and vertical semiaxes of the ellipsoid, whose surface element orientation reflects the phytoelement angle distribution. The function diagram is shown in Fig. 7, b. Orientation of leaves in terms of horizontal direction also has certain peculiarities (Fig. 7, a). A big fraction of NE- and SW-oriented phytoelements is observed. SE quarter is well-represented at the site

U2017-3, NW direction is more frequent in the case of U2016-8 compared to other sites.

A series of polygonal models in a form suitable for ecological tasks has been developed on the basis of point clouds obtained from two-dimensional images (photographs) of the cover fragments (Fig. 8). In particular, Fig. 8, b provides a graphic visualisation of the polygonal model describing the vegetation in the Y-Plant format, which is used for modelling solar radiation absorption (Percy et al. 2011).

Discussion

Relying on the data obtained, we can draw the preliminary conclusion that the presence of *Carex rariflora* in the cover contributes to flattening the distribution density curve, while *Equisetum* increases its slope. At site U2016-1, where the examined layer is dominated by *Carex rariflora* sedge but also has vertically oriented *Equisetum* stems, the simultaneous impact of these two factors results in some intermediate distribution shape.

The sites of sedge tundras thus differ in dominant orientation of the phytoelements, which can be attributed to the species composition of the available communities and to the variable length of phytoelements. The impact of these differences on the emissive and reflective properties of the vegetation

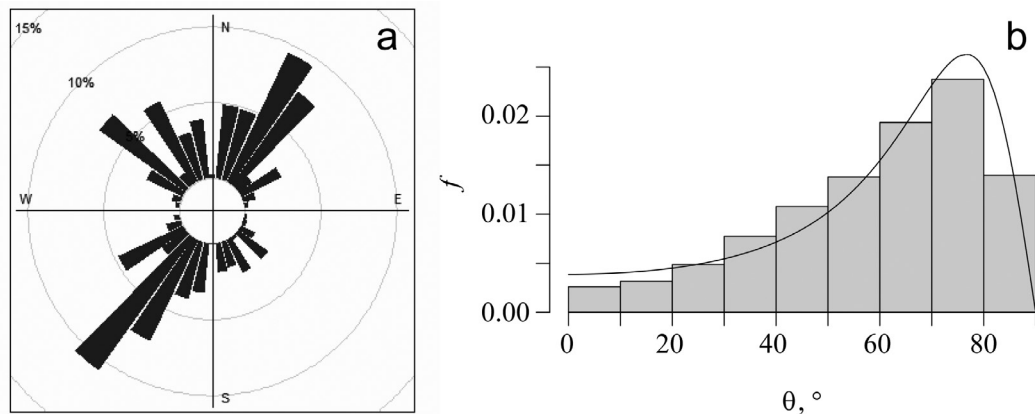


Fig. 7. Generalised description of the phytoelements orientation in the sedge-dwarf-shrub layer of the vegetation cover: a – by phytoelement exposure plot (polar plot with frequencies of certain angle values cumulated radially), b – by phytoelement angle distribution (histogram with a superimposed probability density plot $f(\theta)$, set by a rotated ellipsoidal angle density function with parameter $\chi = 2.69$)

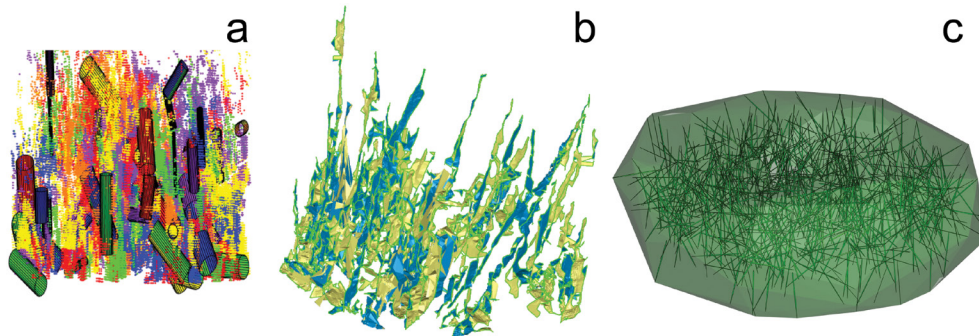


Fig. 8. 3D models of the vegetation cover fragments: a – complex point-polygonal model with phytoelements fitted by cylinders, b – polygonal model with thin plate phytoelement representation, c – polygonal model in Y-Plant format

cover has yet to be evaluated during future studies. No distinct regional features of phytoelement angle distribution have been identified for similar plant communities based on the data for the Nenets Autonomous Area and the Murmansk Region. The actual distribution shape for the surveyed sites differs from the shapes typical of a number of widely used distributions, which raises the question of the limits of the latter's applicability for modelling the matter and energy balance in the ground–vegetation–atmosphere system.

The analytical description of the phytoelement angle distribution with rotated-ellipsoidal function with a set parameter value, which showed the best results in χ^2 test among other descriptions, can be used for a generalised description of the vegetation cover structure of sedge tundras sites for which we have no information on the species composition of the available communities (e. g., when modelling the interaction of electromagnetic radiation with ground cover on a regional scale).

We would like to mention that the study (Juszk et al. 2017) contains an assessment of the phytoelement angle distribution for other species dominant in a number of communities at Eurasian tundra sites for the purposes of modelling radiation emissions. The studied species of sedge vegetation include *Eriophorum angustifolium* and *Eriophorum vaginatum*. Phytoelement angle distributions in a photosynthetically active layer of the cover formed by them are close to those obtained in the current study (the distribution has erectophile and spherical features). Yet the ap-

proximation of actual distributions in the mentioned study was performed by means of the beta-function, which is less efficient in this case in terms of data description than the rotated-ellipsoidal function (χ^2 is about 17 when applying beta-function approximation to the survey data versus 5 when using rotated-ellipsoidal approximation).

The vegetation cover descriptions obtained in this study with various forms of structure data representation may be used to fulfil a wide range of tasks. The obtained spatial polygonal models in the form of coordinated element sets are suitable for modelling absorption and scattering of electromagnetic waves of the optical range in the vegetation layer. The microwave radiation transfer model proposed in study (Huang et al. 2016) can account for the actual cover structure by using the data obtained on phytoelement angle distribution for calculating scattering amplitude tensor elements.

In conclusion, we would like to emphasise that the hardware and software system made it possible partially to make up for the lack of data on the 3D structure of the vegetation cover in the south tundra subzone and lay the foundations for similar surveys on the European territories of Russia. As a result of this study, we have obtained previously unavailable quantitative assessments of the structure parameters and spatial models of the cover fragments for sites occupied by communities with dominating sedges in the sedge-dwarf-shrub layer.

The study was supported by the Russian Foundation for Basic Research (Project No. 16-35-00255 mol-a).

References

- Greaves HE, Vierling LA, Eitel JU, Boelman NT, Magney TS, Prager CM, Griffin KL (2015) Estimating aboveground biomass and leaf area of low-stature Arctic shrubs with terrestrial LiDAR. *Remote Sensing of Environment* 164: 26–35. <https://doi.org/10.1016/j.rse.2015.02.023>
- Huang H, Liao TH, Tsang L, Njoku EG, Colliander A, Jackson T, Yueh S (2016) Combined active and passive microwave remote sensing of soil moisture for vegetated surfaces at L-band. *Geoscience and Remote Sensing Symposium (IGARSS)*, 1626–1629. <https://doi.org/10.1109/IGARSS.2016.7729415>
- Jackson TJ, Schmugge TJ (1991) Vegetation effects on the microwave emission of soils. *Remote Sensing of Environment* 36(3): 203–212. [https://doi.org/10.1016/0034-4257\(91\)90057-D](https://doi.org/10.1016/0034-4257(91)90057-D)
- Juszak I, Erb AM, Maximov TC, Schaepman-Strub G (2014) Arctic shrub effects on NDVI, summer albedo and soil shading. *Remote Sensing of Environment* 153: 79–89. <https://doi.org/10.1016/j.rse.2014.07.021>
- Juszak I, Iturrate-Garcia M, Gastellu-Etchegorry JP, Schaepman ME, Maximov TC, Schaepman-Strub G (2017) Drivers of shortwave radiation fluxes in Arctic tundra across scales. *Remote Sensing of Environment*. 193: 86–102. <https://doi.org/10.1016/j.rse.2017.02.017>
- Magney TS, Eitel JU, Griffin KL, Boelman NT, Greaves HE, Prager CM, et al. (2016) LiDAR canopy radiation model reveals patterns of photosynthetic partitioning in an Arctic shrub. *Agricultural and Forest Meteorology* 221: 78–93. <https://doi.org/10.1016/j.agrformet.2016.02.007>
- Matelenok IV, Melentyev VV (2016) Instrument for investigating of the spatial structure of forest ground covers. In: *Aerospace Methods and GIS-Technologies in Forestry, Forest Management and Ecology*. Proc. 6th All-Russian Conf. Moscow: 138–143.
- Matelenok IV, Melentyev VV (2018) Investigation of 3D structure of vegetation cover in yernik tundra using photography and automated image processing techniques. *Current Problems in Remote Sensing of the Earth from Space* 15(2): 100–111. <https://doi.org/10.21046/2070-7401-2018-15-2-100-111>
- Pearcy RW, Duursma RA, Falster DS (2011) Studying plant architecture with Y-plant and 3D digitising. *PrometheusWiki*. <http://prometheuswiki.publish.csiro.au/tiki-index.php?page=Studying+plant+architecture+with+Y-plant+and+3D+digitising>
- Pisek J, Ryu Y, Alikas K (2011) Estimating leaf inclination and G-function from leveled digital camera photography in broadleaf canopies. *Trees* 25(5): 919–924. <https://doi.org/10.1007/s00468-011-0566-6>
- Thomas SC, Winner WE (2000) A rotated ellipsoidal angle density function improves estimation of foliage inclination distributions in forest canopies. *Agricultural and Forest Meteorology* 100(1): 19–24. [https://doi.org/10.1016/S0168-1923\(99\)00089-1](https://doi.org/10.1016/S0168-1923(99)00089-1)
- Wang WM, Li ZL, Su HB Comparison of leaf angle distribution functions: effects on extinction coefficient and fraction of sunlit foliage. *Agricultural and Forest Meteorology* 143(1): 106–122. <https://doi.org/10.1016/j.agrformet.2006.12.003>
- Zou X, Mottus M, Tammeorg P, Torres CL, Takala T, Pisek J, Makela P, Stoddard FL, Pellikka P (2014) Photographic measurement of leaf angles in field crops. *Agricultural and Forest Meteorology* 184: 137–146. <https://doi.org/10.1016/j.agrformet.2013.09.010>